

Homozygous R136S mutation in PRNP gene causes recessive inherited early onset prion disease

Teresa Ximelis

Hospital Clinic IDIBAPS Neurological Tissue Biobank: Biobanc de l'Hospital Clinic IDIBAPS

Alba Marín-Moreno

CISA: Centro de Investigacion en Sanidad Animal

Juan Carlos Espinosa

CISA: Centro de Investigacion en Sanidad Animal

Hasier Eraña

CIC bioGUNE: Center for Cooperative Research in Biosciences

Jorge M Charco

CIC bioGUNE: Center for Cooperative Research in Biosciences

Isabel Hernández

Fundació ACE: Fundacio ACE

Carmen Riveira

Hospital de León: Complejo Asistencial Universitario de Leon

Daniel Alcolea

Hospital de la Santa Creu i Sant Pau

Eva González-Roca

Hospital Clinic de Barcelona

Iban Aldecoa

Hospital Clinic de Barcelona

Laura Molina-Porcel

Hospital Clinic de Barcelona

Piero Parchi

IRCCS Istituto Delle Scienze Neurologiche di Bologna

Marcello Rossi

IRCCS Istituto Delle Scienze Neurologiche di Bologna

Joaquín Castilla

CIC bioGUNE: Center for Cooperative Research in Biosciences

Raquel Ruiz-García

Hospital Clinic de Barcelona

Ellen Gelpi

Medical University of Vienna: Medizinische Universität Wien

Juan María Torres

CISA: Centro de Investigacion en Sanidad Animal

Raquel Sanchez-Valle (✉ rsanchez@clinic.cat)

Hospital Clinic de Barcelona <https://orcid.org/0000-0001-7750-896X>

Research

Keywords: gene PRNP, GSS, homozygous, neuropathology, prion

Posted Date: May 6th, 2021

DOI: <https://doi.org/10.21203/rs.3.rs-483825/v1>

License: © ⓘ This work is licensed under a Creative Commons Attribution 4.0 International License.

[Read Full License](#)

Homozygous R136S mutation in *PRNP* gene causes recessive inherited early onset prion disease

Teresa Ximelis,^{1,†} Alba Marín-Moreno,^{2,†} Juan Carlos Espinosa,² Hasier Eraña,³ Jorge M Charco,³ Isabel Hernández,⁴ Carmen Riveira,⁵ Daniel Alcolea,⁶ Eva González-Roca,⁷ Iban Aldecoa,^{1,8} Laura Molina-Porcel,^{1,9} Piero Parchi,^{10,11} Marcello Rossi,¹¹ Joaquín Castilla,^{3,12} Raquel Ruiz-García,^{7,9} Ellen Gelpi,^{1,13} Juan María Torres,^{2*} Raquel Sánchez-Valle.^{1,9*}

† **These authors contributed equally to this work.**

Author affiliations:

1 Neurological Tissue Bank of the Biobanc-Hospital Clinic-Institut d'Investigacions Biomediques August Pi i Sunyer (IDIBAPS), 08036 Barcelona, Spain

2 Centro de Investigación en Sanidad Animal (CISA-INIA), 28130 Valdeolmos, Madrid, Spain.

3 Center for Cooperative Research in Biosciences (CIC bioGUNE), Basque Research and Technology Alliance (BRTA), Bizkaia Technology Park, 48160 Derio, Spain

4 Fundació ACE, Barcelona Alzheimer Treatment and Research Center, 08028 Barcelona, Spain

5 Neurology Service, Hospital de León, 24071 León, Spain

6 Memory Unit, Hospital de la Santa Creu i Sant Pau, 08041 Barcelona, Spain

7 Immunology department, Biomedical Diagnostic Center, Hospital Clínic de Barcelona, 08036 Barcelona, Spain

8 Pathology department, Biomedical Diagnostic Center, Hospital Clínic de Barcelona, University of Barcelona, 08036 Barcelona, Spain

23 9 Alzheimer's disease and other cognitive disorders unit. Neurology Service. Hospital Clínic
24 de Barcelona, IDIBAPS, University of Barcelona, 08036 Barcelona, Spain

25 10 Department of Experimental, Diagnostic and Specialty Medicine (DIMES), University of
26 Bologna, 40138 Bologna, Italy.

27 11 IRCCS, Istituto delle Scienze Neurologiche di Bologna, 40139 Bologna, Italy

28 12 IKERBasque Basque Foundation for Science, 48009 Bilbao, Spain

29 13 Division of Neuropathology and Neurochemistry, Department of Neurology, Medical
30 University of Vienna, 1090 Vienna, Austria

31

32 Correspondence to:

33 Raquel Sánchez-Valle

34 Alzheimer's disease and other cognitive disorders unit

35 Neurology Service

36 Hospital Clínic de Barcelona, IDIBAPS, University of Barcelona

37 Villarroel, 170 08036 Barcelona (Spain)

38 +34-932275785

39 rsanchez@clinic.cat

40

41 Juan María Torres

42 Centro de Investigación en Sanidad Animal (CISA-INIA)

43 28130, Valdeolmos, Madrid, Spain

44 jmtorres@inia.es

45 **Word count:**

46 Abstract: 307 words

47 Main Manuscript: 4184 words

48 Tables: 1

49 Figures: 6

50 References: 41

51 **Abstract**

52 **Background:** More than 40 pathogenic heterozygous *PRNP* mutations causing inherited
53 prion diseases have been identified to date. Recessive inherited prion disease has not been
54 described to date.

55 **Methods:** We describe the clinical and neuropathological data of inherited early-onset prion
56 disease caused by the rare *PRNP* homozygous mutation R136S. *In vitro* PrP^{Sc} propagation
57 studies were performed using recombinant-adapted Protein Misfolding Cyclic Amplification
58 technique. Brain material from two R136S homozygous patients were intracranially
59 inoculated in TgMet129 and TgVal129 transgenic mice to assess the transmissibility of this
60 rare inherited form of prion disease.

61 **Results:** The index case presented symptoms of early-onset dementia beginning at the age of
62 49 and died at the age of 53. Neuropathological evaluation of the proband revealed abundant
63 multicentric PrP plaques and Western blotting revealed a 6-8 kDa protease-resistant,
64 unglycosylated PrP fragment, consistent with a Gerstmann-Sträussler-Scheinker phenotype.
65 Her youngest sibling suffered from progressive cognitive decline, motor impairment and
66 myoclonus with onset in her late 30s and died at the age of 48. Genetic analysis revealed the
67 presence of the R136S mutation in homozygosis in the two affected subjects linked to
68 homozygous methionine at codon 129. One sibling carrying the heterozygous R136S
69 mutation, linked to homozygous methionine at codon 129, is still asymptomatic at the age of
70 74. The inoculation of human brain homogenates from our index case and an independent
71 case from a Portuguese family with the same mutation in transgenic mice expressing human
72 PrP and *in vitro* propagation of PrP^{Sc} studies failed to show disease transmissibility.

73 **Conclusion:** In conclusion, biallelic R136S substitution is a rare variant that produces
74 inherited early-onset human prion disease with a Gerstmann-Sträussler-Scheinker

75 neuropathological and molecular signature. Even if the R136S variant is predicted to be
76 “probably damaging”, heterozygous carriers are protected, at least from an early onset
77 providing the first evidence for a recessive pattern of inheritance in human prion diseases.

78 **Keywords:** gene *PRNP*; GSS; homozygous; neuropathology; prion

79 **Background**

80 Genetic prion diseases represent ~15% of human prion diseases [1] and are caused by genetic
81 variants in the *PRNP* gene, located on the chromosome 20. More than 40 rare variants have
82 been described to cause genetic prion disease. Importantly, these mutations are linked to the
83 polymorphism at codon 129, coding either for methionine or valine, which frequently
84 determines the phenotypic presentation. Genetic prion diseases usually present family history
85 of disease. However in some genetic cases, the familial tree [2] could not identify other cases
86 in the family or suggests incomplete penetrance, which has been attributed to underdiagnosis
87 or low clinical expression during the lifespan [3,4]. Mutations induce misfolding of the
88 cellular prion protein (PrP^C), and the accumulation of the disease associated isoform PrP^{Sc}
89 [5,6]. According to the clinic-neuropathological features, inherited prion diseases can be
90 classified as genetic Creutzfeldt-Jakob disease, Gerstmann-Sträussler-Scheinker (GSS)
91 syndrome, Fatal Familial Insomnia and Prion diseases associated to octapeptide insertions
92 although there are also some variants presenting an intermediate clinical phenotype or not
93 fitting into these categories.⁷ The clinical diagnosis of genetic prion disorders might be
94 challenging, especially in patients with non-prototypical phenotypes. Analysis of the human
95 *PRNP* gene is recommended whenever such as disease form is suspected [8,9].

96 Up to date, all described pathogenic variants cause the disease in heterozygous carriers, being
97 the disease inherited with an autosomal dominant pattern. Very few individuals have been
98 reported to be homozygous for *PRNP* variants [10-13]. Most of them are homozygous
99 carriers of well-known pathogenic mutations which cause also the disease in heterozygous
100 carriers from areas of high prevalence of the mutation. In 2006, Pacheco et al. [14] reported
101 at the Prion 2006 meeting a Portuguese patient carrying the homozygous R136S variant with
102 family history of disease in two siblings, but not additional information is available in the
103 literature.

104 In this report, we describe the clinical, neuropathological and biochemical phenotype of
105 genetic prion disease associated with a biallelic R136S substitution in the *PRNP* gene in a
106 Spanish family. We also present the results of *in vivo* and *in vitro* transmissibility and
107 propagation studies of this rare variant.

108 **Materials and methods**

109 **Clinical data**

110 The index case and two asymptomatic siblings were studied at the Alzheimer's disease and
111 other cognitive disorders unit at Hospital Clínic de Barcelona, Barcelona, Spain. Clinical
112 information also included data from other centres specialized in cognitive disorders where the
113 patient was evaluated and followed after diagnosis. The youngest sister and affected patient
114 was examined at Hospital of Leon, Leon, Spain. The clinical information associated with
115 other members of the family was obtained from medical records or was provided by the
116 family members themselves.

117 **Genetic studies**

118 *PRNP* exon 2 was amplified by PCR of genomic DNA extracted from whole peripheral blood
119 as previously described [15] at Hospital Clínic de Barcelona. We used two pathogenic
120 prediction softwares: SIFT [16] and Polymorphism Phenotyping v2 (Polyphen-2 (score 1.0))
121 [17] to predict the potential pathogenic effect of the observed variant. Copy number variation
122 analysis was performed using Affymetrix SNP6.0 arrays.

123 **Neuropathology and immunoblotting**

124 Neuropathologic examination was performed according to standardized protocols at
125 Neurological Tissue Bank of Hospital Clínic-IDIBAPS in Barcelona, Spain. Right brain

126 hemisphere was dissected in coronal sections and frozen while left brain hemisphere was
127 fixed by immersion in 4% formalin for three weeks and after fixation and cutting were treated
128 with 98% formic acid for one hour. Upon several water washes, brain material covering at
129 least 30 different brain areas was postfixed in 10% formalin for at least 48 hours and
130 embedded in paraffin. For histologic evaluation, 5-um-thick sections were stained with
131 hematoxylin & eosin and Periodic Acid-Schiff (PAS). Immunohistochemistry (IHC) was
132 performed using the Autostainer System method (Dako) with various antibodies including
133 anti-PrP (12F10; Bertin-bioreagent, France), anti- β A4 (6F/3D, Dako, Glostrup, Denmark),
134 anti-tau (AT8; Thermo Scientific, USA), anti- α -synuclein (5G4; Analytik Jena, Germany),
135 anti-ubiquitin (P4D1; Cell signalling, USA), anti- α -internexin (2E3, Invitrogen, USA) and
136 anti-TDP-43 (2E2-D3, Abnova, Taiwan). Disease evaluation was performed according to
137 international consensus criteria [18].

138 Samples of frontal, temporal, parietal and occipital cortices, hypothalamus, thalamus and
139 cerebellum were processed for Western Blotting. Human brain tissue was homogenized in
140 10% (w/v) in lysis buffer (100 mM NaCl, 10 mM EDTA, 0.5% Nonidet P-40, 0.5% sodium
141 deoxycholate, 100 mM Tris) at pH 6.9. To detect brain PrP^{res} brain homogenate were
142 subjected to digestion with 2 U/ml of proteinase K (PK) (Roche Diagnostics) at 37°C for 1
143 hour. After blocking PK activity with phenylmethylsulfonyl fluoride (PMSF, final
144 concentration 3.6 mM), samples were boiled in sample buffer (final concentration: 3% SDS,
145 4% β -mercaptoethanol, 10% glycerol, 2 mM EDTA, 62.5 mM Tris) for 6 min at 100 °C.
146 Digested samples were loaded into 12% Tris-Glycine gel (Criterion, Bio-Rad). After
147 electrophoretic transference of proteins onto polyvinylidene fluoride membranes (Bio-Rad)
148 and after blocking the membrane 1 hour at 37°C. After electrophoretic transference of
149 proteins onto polyvinylidene fluoride membranes (Bio-Rad) membranes were incubated with
150 3F4 (1:30.000; Millipore). 3F4 recognizes the 109-112 epitope of the human-PrP^C sequence.

151 Immunocomplexes were detected by 1 hour membrane incubation with horseradish
152 peroxidase conjugated antimouse IgG (GE Healthcare Amersham Biosciences) and
153 development with enhanced chemiluminescence in ECL Select (GE Healthcare Amersham
154 Biosciences). For PrP^{Sc} deglycosylation, N-Linked glycans were removed by using a peptide-
155 N-glycosidase (PNGaseF+) F kit (New England Biolabs) according to the manufacturer's
156 instructions.

157 ***In vitro* propagation of PrP by PMCA**

158 In vitro PrP^{Sc} propagation studies were performed at the Prion Research Lab at CICbioGune,
159 in Bizkaia, Spain. Two different type of experiments were performed using recombinant-
160 adapted Protein Mysfolding Cyclic Amplification (recPMCA) technique as previously
161 described [19]. In the experiment focused on the in vitro propagation of human rec-PrP^{Sc}
162 using R136 vs. S136 human rec-PrP as substrates, samples were complemented with chicken
163 brain homogenate and seeded with different dilutions of recPMCA-adapted CJD MM1
164 misfolded rec-PrP^{Sc} and subjected to a unique 24 h round of standard recPMCA. The
165 experiment focused on the evaluation of the spontaneous propensity to misfold of the R136S
166 variant, was performed twice in duplicates of four and compared with other human mutated
167 rec-PrP and wt rec-PrP. Samples were subjected to 15 rounds of recPMCA [20]. Amplified
168 samples were digested with 50-80 µg/ml of PK and analyzed by western blot using
169 monoclonal antibody D18 (1:5,000).

170 **Transmission studies in human PrP transgenic mice**

171 Inoculation of transgenic mice was performed at Centro de Investigación en Sanidad Animal
172 (CISA-INIA), Madrid, Spain. Inocula were prepared from fresh frozen cerebellar tissue from
173 the proband and from one independent case from the Portuguese family [14] carrying the
174 homozygous R136S variant, as 10% (wt/vol) homogenates in 5% glucose distilled water.

175 Two different mouse models for human-PrP were inoculated: HuPrP-Tg340-Met129
176 (TgMet129) mouse line expressing the Met129-PrP^C variant [21] and HuPrP-Tg362-Val129
177 mouse line expressing the Val129-PrP^C variant (TgVal129) [22]. These transgenic mouse
178 lines express 4-fold and 8-fold the level of PrP^C expression in human brain respectively. Six
179 to nine individually identified mice 6–10-week-old were anesthetized and inoculated with 2
180 mg of 10% brain homogenate in the right parietal lobe by using a 25-gauge disposable
181 hypodermic needle. After inoculation, mice were observed daily and their neurologic status
182 was assessed weekly. At the established experimental endpoint (700 days postinoculation),
183 animals were euthanized. After necropsy, part of the brain was fixed by using immersion in
184 neutral-buffered 10% formalin (4% 2-formaldehyde) and used it for histopathology analysis
185 while the rest of the tissue was frozen at -20°C and used for proteinase K-resistant PrP^{Sc}
186 (PrP^{res}) detection by WB. For each inoculation experiment, mean survival times with standard
187 deviation was calculated as well as the attack rate defined as the proportion of mice that
188 scored positive for PrP^{res} divided by the number of total inoculated mice.

189 **Western blotting in mouse bioassay**

190 Western blotting analysis was done as previously described [23]. Briefly, 175 + 20 mg of
191 frozen mouse brain tissue were homogenized in 5% glucose distilled water in grinding tubes
192 (Bio-Rad) and adjusted to 10% (wt/vol) by using a TeSeE Precess 48TM homogenizer (Bio-
193 Rad). To detect brain PrP^{res} 100 µL of 10% (wt/vol) brain homogenate were subjected to
194 digestion with 40 µg/mL of PK in buffer 5% sarkosyl, 5% Triton X100, 1 M Urea and 16
195 mM Tris-HCl (pH 9.6) at 60 °C for 15 min. Digested samples were loaded samples into 12%
196 Bis-Tris Gel (Criterion XT; Bio-Rad). After electrophoretic transference of proteins onto
197 polyvinylidene fluoride membranes (Millipore) and blocking overnight with 2% bovine
198 serum albumin blocking buffer, membranes were incubated with 12B2 [24] and Sha31 [25]

199 mAb at a concentration of 1 µg/mL. 12B2 recognizes the 89-WGQGG-93 epitope of the
200 human-PrP^C sequence while Sha31 recognizes the 145-WEDRYyre-152 epitope of the
201 human-PrP^C sequence. Immunocomplexes were detected by 1 h membrane incubation with
202 horseradish peroxidase conjugated antimouse IgG (GE Healthcare Amersham Biosciences)
203 and development with enhanced chemiluminescence in ECL Select (GE Healthcare
204 Amersham Biosciences). Images were captured using the ChemiDoc WRS+ System and
205 processed them by using Image Lab 5.2.1 software (both Bio-Rad).

206 **Histological analysis in mouse bioassay**

207 Mouse brain samples were immediately fixed in neutral-buffered 10% formalin (4% 2-
208 formaldehyde) during necropsy, coronally trimmed and processed routinely. After embedded
209 in paraffin-wax, tissues were cut to 4µm thickness, de-waxed and rehydrated by standard
210 procedures. Tissue slides were subjected to two different histological methods:
211 hematoxylin&eosin staining for lesion profile evaluation by standard methods [26] and IHC.
212 Lesion profile evaluation was done by semi-quantitative assessment of spongiform
213 degeneration scoring vacuolization in the following brain areas: cerebral cortex (CCtx);
214 striatum (Stri); hippocampus (Hpp); thalamus (Thal); hypothalamus (Hpth); midbrain (Midb);
215 cerebellar cortex (CbCtx); pons/medulla oblongata (PoMe). For the IHC analysis, tissue
216 slides were subjected to antigen retrieval and quenching of hydrogen peroxide, latter
217 incubated with the Sha31 mAb [25] and subsequent steps of the IHC procedure were
218 performed by a commercial immunoperoxidase technique (Vector-Elite ABC kit, Vector
219 Laboratories) as per manufacturer's instructions finally counterstaining the sections with
220 Harri's haematoxylin.

221 **Results**

222 **Clinical characterization and family history**

223 The index patient was a 51-year-old female who was referred to the Neurology department
224 due to progressive memory decline, language problems and subtle changes in behaviour
225 (apathy and childish behaviour) beginning at the age of 49 years (Table 1, Figure 1A, subject
226 II.5). At first examination, her Minimental State examination Score was 28/30. The cognitive
227 evaluation revealed moderate generalized cognitive impairment including mild verbal
228 memory impairment and visuospatial, language and executive disturbances. The neurological
229 examination was normal except for mild dysarthria. MRI examination was unremarkable
230 (Figure 2). Cerebrospinal fluid showed elevated total tau levels (1262 pg/ml), Abeta42
231 (701pg/ml) within the normal range, slightly elevated phospho-tau (68.5 pg/ml), and reduced
232 p-tau/t-tau ratio (0,054). The 14-3-3 Western-Blot test was negative. The patient deteriorated
233 progressively over the next years with worsening of both cognitive and motor functions
234 developing severe ataxia. She died at the age of 53 after disease duration of 4 years.

235 The youngest sibling of the index patient (Table 1, Figure 1A subject II-6) also suffered from
236 cognitive decline, motor impairment and myoclonus with onset in her late 30s (38 years).
237 Neurological examination, MRI scan and CSF 14-3-3 were normal at first examination, but
238 the disease progressed and the patient was severely impaired after 10 years of disease. The
239 patient died at the age of 48, but the postmortem neuropathological examination was not
240 performed. The other four siblings were neurologically preserved (present ages from 63 to 74
241 years) (Figure 1A, II.1-II.4).

242 The proband's parents were born in a small village in the North-west of Spain, and were
243 probably consanguineous but the degree of kinship is unknown. The mother (Figure 1A,
244 subject I.2) died at the age of 89 years and was neurologically healthy according to their

245 family members. The father (Figure 1A, subject I.1) died at the age of 84 with dementia with
246 a clinical onset at the age of 75 that had been classified as vascular cognitive impairment by
247 the treating physician.

248 **Genetic studies**

249 The genetic study of the Spanish patient and her youngest sister showed the presence of a
250 substitution of guanine for thymine (AGG to AGT) at codon 136 of the *PRNP* in the two
251 alleles, causing the missense mutation R136S in homozygosis. This was linked to methionine
252 homozygosis at codon 129. No deletions or duplications were detected in the 100kb region
253 which includes the *PRNP* gene.

254 Of the four asymptomatic siblings, two underwent genetic testing. One asymptomatic 74-
255 year-old sibling (Figure 1A, subject II.1) carried the R136S mutation in heterozygosis, which
256 was also linked to homozygous methionine at codon 129. Another sibling showed a normal
257 *PRNP* sequence and was also methionine homozygous at codon 129.

258 According to pathogenic prediction software, the R136S variant is considered to be damaging
259 (SIFT) [16], or probably damaging (Polymorphism Phenotyping v2 (Polyphen-2 (score 1.0))
260 [17].

261 **Neuropathological findings and immunoblotting**

262 The brain of the index patient was removed after death at the Neurological Tissue Bank of the
263 IDIBAPS Biobank in Barcelona. Unfixed brain weight was 1030g. Gross examination
264 showed a moderate diffuse brain atrophy accentuated in the frontal lobes and mild nigral
265 pallor. Histology revealed a severe involvement of grey matter that showed prominent
266 neuronal loss, astrogliosis and microglial proliferation, especially in frontal cortex (Figure
267 3A). Despite observing a superficial laminar spongiosis, only mild bona fide spongiform

268 change was detected in grey matter which was characterized by a few small-sized vacuoles in
269 cortical regions and basal ganglia. The most striking feature was the presence of abundant
270 amyloid plaques consisting of multiple densely packed cores (multicentric plaques) that were
271 variably PAS positive and strongly immunoreactive for PrP^{Sc} (12F10 antibody) after
272 pretreating the tissue sections for removal of physiological PrP^C. These multicentric plaques
273 were detected in all cortical areas - with less involvement of primary visual cortex, in basal
274 ganglia, thalamic nuclei, and brainstem and in the molecular layer of cerebellar cortex.
275 Moreover, multicentric PrP amyloid plaques induced a moderate neuritic component that was
276 immunoreactive for phosphorylated tau (AT8).

277 PrP Western blotting displayed a multiple banding pattern with a prominent low molecular
278 weight (mw) fragment of ~8kDa which is absent in the in comparison to the PrP Type 1
279 (sCJDMM1) control sample run in parallel, in which the lowest mw band detected was
280 ~21kDa (Figure 4). The intensity of the bands was variable among different brain regions and
281 after treatment with PNGaseF+. At visual inspection, the frontal cortex contained the highest
282 amounts of PrP^{Sc}.

283 ***In vitro* propagation of PrP^{Sc}**

284 In order to evaluate the effect of the R136S mutation in the in vitro propagation of human
285 rec-PrP^{Sc}, human 129M 136R (wt) rec-PrP, human 129M 136S rec-PrP and a mix of both
286 rec-PrPs in ratio 1:1 were used as substrates for recPMCA and seeded with different dilutions
287 of recPMCA-adapted CJD MM1 misfolded rec-PrP (10⁻¹ – 10⁻⁸), and subjected to a unique
288 24 h round of standard recPMCA. No significant differences were found in the propagation
289 ability of the R136 (wt) vs. the mutant R136S rec-PrP or the mix 1:1 of both proteins.

290 To evaluate the spontaneous propensity of the R136S recPrP to misfold compared to the wt
291 recPrP and other GSS-related mutated recPrP (P105L and A117V), a serial rec-PMCA (15

292 rounds) was performed (Figure 6). All cases were associated with methionine at codon 129.
293 The wt and the R136S PrP linked to the methionine polymorphic variant at codon 129 did not
294 show spontaneous misfolding, in contrast to the other GSS-related recPrP.

295 **Bioassay in human-PrP transgenic mice**

296 Brain material from the two patients (the Spanish index case and the Portuguese index case)
297 were intracranially inoculated in TgMet129 and TgVal129 transgenic mice (Table 2) to
298 assess the transmissibility of this rare inherited form of prion disease. These mouse lines
299 expressed in homozygosis the Met129-PrP^C variant or the Val129-PrP^C variant respectively.
300 All mice were sacrificed at the end of their lifespan without showing any clinical sign
301 suspicious of prion disease and remaining uninfected. No PrP^{res} was found in mice brains
302 either by WB nor IHC (data not shown). Vacuolization was no different from the one
303 associated with the natural aging process of non-inoculated control mice of the same
304 transgenic lines by histology (data not shown).

305 **Discussion**

306 We report here that the biallelic R136S *PRNP* mutation causes inherited human prion disease
307 with early onset of symptoms (30s-40s). The same mutation presented in heterozygous state
308 in other family members did not induce the same phenotype. Clinically, the patients
309 presented with early-onset dementia developing motor disturbances at follow-up.
310 Neuropathological examination revealed the presence of abundant multicentric PrP amyloid
311 plaques with mild neuritic component, along with severe neuronal loss, gliosis and microglial
312 proliferation with only mild spongiform change, which is consistent with a GSS
313 neuropathological phenotype. In contrast to previous description of homozygous mutations in
314 *PRNP* [10-13,27] (Table 1), the disease in R136S families presented with an autosomal

315 recessive pattern of inheritance, keeping the heterozygous family members protected from
316 developing the disease, at least, at early ages. *In vitro* propagation and *in vivo* transmissibility
317 studies suggest that the PrP^{Sc} variant resulting from the R136S mutation failed to propagate
318 both *in vivo* and *in vitro* in the conditions analyzed, suggesting that this variant is biologically
319 less active than other mutations causing genetic prion diseases.

320 Previous described pathogenic mutations cause human prion disease in the heterozygous state
321 and show an autosomal dominant inheritance pattern. There are scarce examples in the
322 literature of patients affected by prion diseases carrying homozygous genetic variants.
323 Homozygous E200K carriers are associated with consanguinity in areas of high prevalence of
324 this variant. Homozygous carriers of the E200K mutation present an earlier age of onset than
325 heterozygous carriers but no other relevant differences in clinical features compared with
326 heterozygous carriers [10]. One case of prion disease linked to homozygous Q212P has been
327 described, but also another case has been reported in a heterozygous carrier [11]. Komatsu et
328 al. [12] reported the case of a homozygous V203I patient, in addition to three previously
329 reported heterozygous patients for this variant. However the lack of family history of disease
330 in all the V203I and the presence of this variant in normal controls suggest that this variant
331 could not be pathogenic [3] and more probably could represent benign variant or “risk”
332 variants that might increase the risk of developing a prion disease [11,27].

333 Minikel et al. [3] reported in 2016 the presence of the R136S variant in heterozygosis in two
334 alleles from 60.706 population control exomes but not in patients, suggesting that this
335 represents a very rare variant in the normal population even if the R136S variant is predicted
336 to be “probably damaging” in several pathogenicity prediction software. In our center, we
337 had not identified this genetic variant in more than 300 Spanish subjects (including both
338 patients and controls) analyzed so far. In 2006, Pacheco et al. [14] described one Portuguese
339 patient (Figure 1B, subject II.1) with similar clinical and neuropathological features of those

340 of our patients (early-onset dementia, motor symptoms in her early 50s and a GSS
341 neuropathological phenotype) linked to the presence of the homozygous R136S variant. Two
342 of her siblings presented history of similar disease in their early 50s, but not the parents who
343 should be obligated carriers.

344 In both families (the present family and the Portuguese family) described heterozygous
345 carriers were apparently protected from disease. As the genetic study in the Portuguese index
346 case's mother (Figure 1B, subject I.2) and another family member neurologically preserved
347 in their 80s and 90s revealed the presence of heterozygous R136S linked to 129MV, the
348 authors suggested that the presence of valine in the trans-allele could prevent the expression
349 of the disease. In contrast, in the Spanish family, one heterozygous carrier, homozygous for
350 methionine at codon 129 is neurologically preserved in their 70s, suggesting that the
351 expression of the disease does not depend on the codon 129 of the trans-allele but in the
352 homozygous state or "dosage" of the mutant allele.

353 The expression of the disease only in homozygous subjects could be explained by a dose
354 effect as it has been suggested for an earlier age of onset in homozygous E200K carriers [10].
355 A larger number of R136S PrP molecules (or the absence of wild-type protein) in the
356 homozygous patient's brain may increase the chance of spontaneous conversion. Even if
357 homozygous patients are at higher risk for the spontaneous conversion to PrP^{Sc} than
358 heterozygous patients, on the other hand, the subsequent infective process based on PrP^{Sc}-
359 PrP^C interaction might be less effective as there is only mutant PrP^{Sc} leading to longer disease
360 duration.

361 Even if we cannot rule-out a late onset of the disease, the presence of known or obligated
362 heterozygous carriers in neurological preserved family members that were already in their
363 70s, 80s or 90s make this possibility much less probable during the usual lifespan. In this

364 sense, we believe that both family trees (Figure 1), provide first evidence for a recessive
365 pattern of inheritance in human prion diseases.

366 The clinical phenotype in the patients resembled that of insertion mutations (OPRI), which
367 are characterized by early-onset progressive dementia with late motor dysfunction [6],
368 whereas the neuropathological features were typical of GSS. The observed clinical phenotype
369 is atypical for GSS, which more commonly present with motor signs followed by dementia,
370 although it has also been linked to other point mutations (Y218N) [6] and OPRI [27,28].
371 Irrespectively of the clinical syndrome and the relative regional distribution of lesions, GSS is
372 defined by the presence of multicentric PrP amyloid plaques in the cerebral and cerebellar
373 cortices [7,18]. In contrast to other human prion diseases, the presence of spongiform change
374 can be variable, from absent to severe, which could explain the lack of signal intensity
375 changes in Diffusion Weighted-Imaging in MRI scans. In addition, western blot studies
376 typically show PK-resistant non-glycosylated PrP^{Sc} fragments with a low molecular weight
377 that oscillates between 6-8kDa depending on the PRNP pathogenic variant. Occasionally,
378 however, the immunoblot profile can also show larger truncated PrP^{res} fragments with a
379 molecular weight of 19-21 kDa, as observed in other sporadic or genetic prion diseases [29-
380 31].

381 Animal modeling of human inherited prion diseases is not easy. Practically all attempts to
382 generate transgenic mouse models for human inherited prion diseases using the human-PrP^C
383 sequence had been unsuccessful apart from the recent reported exception of an A117V GSS
384 model [32]. The rest of successful transgenic mouse models that develop spontaneously
385 neurologic disorders when harboring mutations that have been reported in human inherited
386 prion diseases have been made in mouse or bank vole PrP sequences or in chimeric
387 mouse/human PrP proteins [33]. It seems that mouse and bank vole PrP proteins are more
388 prone to spontaneous misfolding while human PrP is apparently more resistant. Alternatively,

389 interactions between mouse PrP and other than PrP mouse factors may be important for the
390 spontaneous generation of prions. In general terms for GSS modelling, models
391 overexpressing mouse, mouse/human chimeric and cow PrP harboring the respective
392 equivalents to human P102L mutation spontaneously developed a prion disease along with
393 neuropathological changes [33]. However, brain PrP^{res} detection and transmissibility to wild-
394 type mice was only achieved in the particular case of equivalent P113L mutation in cow-PrP^C
395 sequence producing a prion agent with features resembling those of classical bovine
396 spongiform encephalopathy [34]. When the A117V mutation was overexpressed in the mouse
397 sequence (A116V) at 4–6x levels, transgenic mice showed signs of prion disease including
398 neuropathology markers but no PrP^{res} were detected [35]. However, A117V GSS cases were
399 successfully transmitted into A117V human PrP transgenic mice Tg30 and Tg31 (2x and 3x
400 overexpression respectively) [32,36] from which Tg30 developed a spontaneous disease that
401 was later transmissible to both Tg30 and Tg31 mice as well as to wild-type V129 human PrP
402 transgenic mice [32]. It would be of interest to further investigate the effects of this
403 homozygous mutation in an animal model, as well as the production of heterozygous animals
404 to further investigate to which extent the presence of the wild-type allele dampens the
405 spontaneous misfolding of the mutated one. The recessive inheritance pattern displayed by
406 this disease in humans points to a protective effect exerted by the wild-type variant and the *in*
407 *vitro* studies performed in this work also supports this hypothesis. However, a slower
408 misfolding rate of the wild-type allele that may finally contribute to disease development at
409 elder ages cannot be ruled out.

410 However, prion ability to cause direct cellular damage (toxicity) has often been dissociated
411 from the capacity of successfully transmit from an infected host to an uninfected recipient
412 (transmissibility) [37]. This fact, added to the difficulty of modelling inherited prion disease

413 that is further discussed below, may explain the lack of *in vivo* and *in vitro* propagation of the
414 prion disease associated to R136S mutation.

415 This report has some limitations. First, the diagnosis of genetic prion disease is a hurdle task
416 and some members of both extended families might have been underdiagnosed, lowering the
417 possibilities of describing this mutation in other patients. Second, due to the lack of
418 neuropathological evaluation in any of the asymptomatic heterozygous carriers, we could not
419 rule-out subclinical prion disease at late ages, although this possibility seems less probable.

420 **Conclusions**

421 The biallelic R136S substitution is a rare *PRNP* mutation that induces inherited human prion
422 disease presenting with early-onset dementia and motor impairment and neuropathological
423 and molecular features consistent with GSS. Even if the R136S variant is predicted to be
424 “probably damaging”, heterozygous carriers are protected, at least, from an early-onset,
425 providing the first pieces of evidence for a recessive pattern of inheritance in human prion
426 diseases.

427 **Abbreviations**

428 Cellular prion protein: PrP^C ; cerebellar cortex: CbCtx; cerebral cortex: CCtx; Gerstmann-
429 Sträussler-Scheinker: GSS; hippocampus:Hpp; hypothalamus: Hpth; HuPrP-Tg340-
430 Met129:TgMet129; Immunohistochemistry: IHC; midbrain: Midb; neurologically preserved:
431 NP; obligated carrier: OP; Periodic Acid-Schiff: PAS; peptide-N-glycosidase: PNGaseF+;
432 phenylmethylsulfonyl fluoride: PMSF; pons/medulla oblongata: PoMe; Protein Mysfolding
433 Cyclic Amplification: recPMCA; proteinase K: PK; proteinase K-resistant PrP^{Sc}: PrP^{res};
434 striatum: Stri; thalamus: Thal; Val129-PrP^C variant: TgVal129

435 **Acknowledgements**

436 We are indebted to the Neurological Tissue Bank of Hospital Clínic-IDIBAPS Biobank for
437 sample and data procurement. We are grateful with Dr Paula Pacheco, Departamento de
438 Genética Humana, Instituto Nacional de Saúde Doutor Ricardo Jorge, Portugal, and Dr
439 Leonor Orge, Laboratório de Patologia, Instituto Nacional de Investigação Agrária e
440 Veterinária, Portugal, for providing the frozen samples from an affected subject from
441 Portugal for the transmissibility studies.

442 **Author's contributions**

443 RSV and JMT designed the study. AMM, HE, JMC, EG, PP and MR performed experiments.
444 JCE, PP, JC, RRG, EG, JMT and RSV interpreted the results. JCE, HE, JMC, IH, CR, DA,
445 EGR, IA, LMP, PP, MR, RRG and EG contributed to the sample collection and
446 characterization. EG, JMT, JC, LMP and RSV provided extensive feedback to the manuscript
447 to improve it significantly. TX and AMM wrote the manuscript draft. All authors read and
448 approved the final manuscript.

449 **Funding**

450 This work was funded by the Instituto de Salud Carlos III (grant n1 PI20/00448 to RSV),
451 Spanish Ministerio de Ciencia e Innovación (grant no. PDI2019-105837RB-I00 to J.M.T. and
452 J.C.E., and RTI2018-098515-B-I00 to J.C), Fundació La Marató de TV3 (grant no. 201821-
453 31 to J.C.E.) and Instituto Nacional de Investigación y Tecnología Agraria y Agroalimentaria
454 (fellowship INIA-FPI-SGIT-2015-02 to A.M.M.). The funders had no role in study design,
455 data collection and analysis, decision to publish, or preparation of the manuscript.

456 **Availability of data and materials**

457 The datasets used and/or analysed during the current study are available from the
458 corresponding author on reasonable request.

459 **Declarations**

460 **Ethics approval and consent to participate**

461 The study was approved by the ethical committee of the Hospital Clínic de Barcelona.

462 Animal experiments were conducted in accordance with the Code for Methods and Welfare
463 Considerations in Behavioral Research with Animals (Directive 2010/63/EU) and every
464 effort was made to minimize animal suffering. Transmission experiments were developed at
465 Centro de Investigación en Sanidad Animal (CISA-INIA, Madrid, Spain) and they were
466 evaluated by the Committee on the Ethics of Animal Experiments of the Instituto Nacional de
467 Investigación y Tecnología Agraria y Alimentaria and approved by the General Directorate of
468 the Madrid Community Government (permit nos. PROEX 291/19 and PROEX 094/18).

469 **Consent for publication**

470 The participants or their next-of-kin provided written informed consent for the use of samples
471 for diagnostic and research purposes.

472 **Competing interests**

473 RSV reports personal fees from Wave pharmaceuticals and Ionis Pharmaceuticals for
474 attending Advisory board meetings, personal fees from Roche diagnostics, Janssen and
475 Neuraxpharm for educational activities, and research grants to her institution from Biogen
476 and Sage Therapeutics outside the submitted work. The other authors report no competing
477 interests.

478 **Author details**

479 ¹Neurological Tissue Bank of the Biobanc-Hospital Clinic-Institut d'Investigacions
480 Biomediques August Pi i Sunyer (IDIBAPS), 08036 Barcelona, Spain. ²Centro de
481 Investigación en Sanidad Animal (CISA-INIA), 28130 Valdeolmos, Madrid, Spain. ³Center
482 for Cooperative Research in Biosciences (CIC bioGUNE), Basque Research and Technology
483 Alliance (BRTA), Bizkaia Technology Park, 48160 Derio, Spain. ⁴Fundació ACE, Barcelona
484 Alzheimer Treatment and Research Center, 08028 Barcelona, Spain. ⁵Neurology Service,
485 Hospital de León, 24071 León, Spain. ⁶Memory Unit, Hospital de la Santa Creu i Sant Pau,
486 08041 Barcelona, Spain. ⁷Immunology department, Biomedical Diagnostic Center, Hospital
487 Clínic de Barcelona, 08036 Barcelona, Spain. ⁸Pathology department, Biomedical Diagnostic
488 Center, Hospital Clínic de Barcelona, University of Barcelona, 08036 Barcelona, Spain.
489 ⁹Alzheimer's disease and other cognitive disorders unit. Neurology Service. Hospital Clínic
490 de Barcelona, IDIBAPS, University of Barcelona, 08036 Barcelona, Spain. ¹⁰Department of
491 Experimental, Diagnostic and Specialty Medicine (DIMES), University of Bologna, 40138
492 Bologna, Italy. ¹¹IRCCS, Istituto delle Scienze Neurologiche di Bologna, 40139 Bologna,
493 Italy. ¹²IKERBasque Basque Foundation for Science, 48009 Bilbao, Spain. ¹³Division of
494 Neuropathology and Neurochemistry, Department of Neurology, Medical University of
495 Vienna, 1090 Vienna, Austria.

496 **References**

497 1. Head MW, Ironside JW, Ghetti B, et al. Prion diseases. In: Love S, Budka H, Ironside
498 JW, Perry A, eds. Greenfield's Neuropathology. 9th ed. Boca Raton, FL: CRC Press;
499 2015:1016–1086.

- 500 2. Budka H, Aguzzi A, Brown P, et al. Neuropathological diagnostic criteria for
501 Creutzfeldt-Jakob disease (CJD) and other human spongiform encephalopathies (prion
502 diseases). *Brain Pathol.* 1995;5(4):459-466. doi: 10.1111/j.1750-3639.1995.tb00625.x.
503 PMID: 8974629.
- 504 3. Minikel EV, Vallabh SM, Lek M, et al. Quantifying prion disease penetrance using
505 large population control cohorts. *Sci Transl Med.* 2016;8(322):322ra9. doi:
506 10.1126/scitranslmed.aad5169. PMID: 26791950; PMCID: PMC4774245.
- 507 4. Kovács GG, Puopolo M, Ladogana A, et al. Genetic prion disease: the EUROCCJ
508 experience. *Hum Genet.* 2005;118(2):166-174. doi: 10.1007/s00439-005-0020-1. Epub 2005
509 Nov 15. PMID: 16187142.
- 510 5. Kovács GG. Genetic background of human prion diseases. 2007;60(11-12):438-446.
511 Hungarian. PMID: 18198790.
- 512 6. Alzualde A, Indakoetxea B, Ferrer I, et al. A novel PRNP Y218N mutation in
513 Gerstmann-Sträussler-Scheinker disease with neurofibrillary degeneration. *J Neuropathol*
514 *Exp Neurol.* 2010;69(8):789-800. doi: 10.1097/NEN.0b013e3181e85737. PMID: 20613639.
- 515 7. Ritchie DL. Chapter Fourteen - Neuropathology of Human Prion Diseases, Editor(s):
516 Giuseppe Legname, Silvia Vanni. *Progress in Molecular Biology and Translational*
517 *Science, Academic Press, Volume 150, 2017, Pages 319-339.* doi:
518 10.1016/bs.pmbts.2017.06.011. Epub 2017 Aug 3. PMID: 28838666.
- 519 8. Brown P, Cathala F, Castaigne P, et al. Creutzfeldt-Jakob disease: clinical analysis of
520 a consecutive series of 230 neuropathologically verified cases. *Ann Neurol.* 1986;20(5):597-
521 602. doi:10.1002/ana.410200507. doi: 10.1002/ana.410200507. PMID: 3539001.
- 522 9. Windl O, Dempster M, Estibeiro JP, et al. Genetic basis of Creutzfeldt-Jakob disease
523 in the United Kingdom: a systematic analysis of predisposing mutations and allelic variation

524 in the PRNP gene. *Hum Genet.* 1996;98(3):259-264. doi: 10.1007/s004390050204. PMID:
525 8707291.

526 10. Simon ES, Kahana E, Chapman J, et al. Creutzfeldt-Jakob disease profile in patients
527 homozygous for the PRNP E200K mutation. *Ann Neurol.* 2000;47(2):257-260. PMID:
528 10665501.

529 11. Beck JA, Poulter M, Campbell TA, et al. PRNP allelic series from 19 years of prion
530 protein gene sequencing at the MRC Prion Unit. *Hum Mutat.* 2010;31(7):E1551-E1563. doi:
531 10.1002/humu.21281. PMID: 20583301.

532 12. Komatsu J, K. Sakai, T. Hamaguchi, et al. Creutzfeldt-Jakob disease associated with a
533 V203I homozygous mutation in the prion protein gene. *Prion* 8, 336–338 (2014). doi:
534 10.4161/19336896.2014.971569. PMID: 25495585; PMCID: PMC4601383.

535 13. Nitsan Z, Cohen OS, Chapman J, et al. Familial Creutzfeldt-Jakob disease
536 homoasanteasantzygous to the E200K mutation: clinical characteristics and disease course. *J*
537 *Neurol.* 2020 Aug;267(8):2455-2458. doi: 10.1007/s00415-020-09826-z. Epub 2020 May 4.
538 PMID: 32367297.

539 14. Pacheco P, Orge L, Head H, et al. Novel prion disease mutation R136S has an
540 incomplete penetrance dependent upon codon 129 trans allele. Abstract from Prion 2006:
541 Strategies, advances and trends towards protection of society, Turin, Italy.

542 15. Sanchez-Valle R, Nos C, Yagüe J, et al. Clinical and genetic features of human prion
543 diseases in Catalonia. *Eur J Neurol* 2004; 11:649-55. doi: 10.1111/j.1468-1331.2004.00967.x.
544 PMID: 15469448.

545 16. Kumar P, Henikoff S, Ng PC. Predicting the effects of coding non-synonymous
546 variants on protein function using the SIFT algorithm. *Nat Protoc.* 2009;4(7):1073-81. doi:
547 10.1038/nprot.2009.86. Epub 2009 Jun 25. PMID: 19561590.

- 548 17. Adzhubei IA, Schmidt S, Peshkin L, et al. *Nat Methods* 7(4):248-249 (2010). doi:
549 10.1038/nmeth0410-248. PMID: 20354512; PMCID: PMC2855889.
- 550 18. Parchi P, de Boni L, Saverioni D, et al. Consensus classification of human prion
551 disease histotypes allows reliable identification of molecular subtypes: an inter-rater study
552 among surveillance centres in Europe and USA. *Acta Neuropathol.* 2012. Oct;124(4):517-
553 29. doi: 10.1007/s00401-012-1002-8. Epub 2012 Jun 30. PMID: 22744790; PMCID:
554 PMC3725314.
- 555 19. Elezgarai SR, Fernández-Borges N, Eraña H, et al. Generation of a new infectious
556 recombinant prion: a model to understand Gerstmann-Sträussler-Scheinker syndrome. *Sci*
557 *Rep.* 2017 Aug 29;7(1):9584. doi: 10.1038/s41598-017-09489-3. PMID: 28851967; PMCID:
558 PMC5575253.
- 559 20. Lund C, Olsen CM, Tveit H, Tranulis MA. Characterization of the prion protein 3F4
560 epitope and its use as a molecular tag. *J Neurosci Methods.* 2007 Sep 30;165(2):183-90. doi:
561 10.1016/j.jneumeth.2007.06.005. Epub 2007 Jun 13. PMID: 17644183.
- 562 21. Padilla D, Béringue V, Espinosa JC, et al. Sheep and goat BSE propagate more
563 efficiently than cattle BSE in human PrP transgenic mice. *PLoS Pathog.* 2011
564 Mar;7(3):e1001319. doi: 10.1371/journal.ppat.1001319. Epub 2011 Mar 17. PMID:
565 21445238; PMCID: PMC3060172.
- 566 22. Notari S, Xiao X, Espinosa JC, et al. Transmission characteristics of variably
567 protease-sensitive prionopathy. *Emerg Infect Dis.* 2014 Dec;20(12):2006-14. doi:
568 10.3201/eid2012.140548. PMID: 25418590; PMCID: PMC4257788.
- 569 23. Aguilar-Calvo P, Espinosa JC, Andréoletti O, et al. Goat K222-PrPC polymorphic
570 variant does not provide resistance to atypical scrapie in transgenic mice. *Vet Res.* 2016 Sep
571 22;47(1):96. doi: 10.1186/s13567-016-0380-7. PMID: 27659200; PMCID: PMC5034450.

- 572 24. Yull HM, Ritchie DL, Langeveld JP, et al. Detection of type 1 prion protein in variant
573 Creutzfeldt-Jakob disease. *Am J Pathol.* 2006 Jan;168(1):151-7. doi:
574 10.2353/ajpath.2006.050766. PMID: 16400018; PMCID: PMC1592651.
- 575 25. Féraudet C, Morel N, Simon S, et al. Screening of 145 anti-PrP monoclonal
576 antibodies for their capacity to inhibit PrPSc replication in infected cells. *J Biol Chem.* 2005
577 Mar 25;280(12):11247-58. doi: 10.1074/jbc.M407006200. Epub 2004 Dec 23. PMID:
578 15618225.
- 579 26. Fraser H, Dickinson AG. Studies of the lymphoreticular system in the pathogenesis of
580 scrapie: the role of spleen and thymus. *J Comp Pathol.* 1978 Oct;88(4):563-73. doi:
581 10.1016/0021-9975(78)90010-5. PMID: 101558.
- 582 27. Goldfarb LG, Brown P, Vrbovska A, et al. An insert mutation in the chromosome 20
583 amyloid precursor gene in a Gerstmann-Sträussler-Scheinker family. *J Neurol Sci.* 1992
584 Sep;111(2):189-94. doi: 10.1016/0022-510x(92)90067-u. PMID: 1431985.
- 585 28. Kovács GG, Trabattoni G, Hainfellner JA, et al. Mutations of the prion protein gene
586 phenotypic spectrum. *J Neurol.* 2002 Nov;249(11):1567-82. doi: 10.1007/s00415-002-0896-
587 9. PMID: 12420099.
- 588 29. Gambetti P, Kong Q, Zou W, Parchi P, Chen SG. Sporadic and familial CJD:
589 classification and characterisation. *Br Med Bull.* 2003;66:213-239. doi:
590 10.1093/bmb/66.1.213. PMID: 14522861.
- 591 30. Rossi M, Baiardi S, Parchi P. Understanding Prion Strains: Evidence from Studies of
592 the Disease Forms Affecting Humans. *Viruses.* 2019;11(4):309. doi: 10.3390/v11040309.
593 PMID: 30934971; PMCID: PMC6520670.

- 594 31. Pirisinu L, Di Bari MA, D'Agostino C, et al. Gerstmann-Sträussler-Scheinker disease
595 subtypes efficiently transmit in bank voles as genuine prion diseases. *Sci Rep.* 2016;6:20443.
596 Published 2016 Feb 4. doi: 10.1038/srep20443. PMID: 26841849; PMCID: PMC4740801.
- 597 32. Asante EA, Linehan JM, Tomlinson A, et al. Spontaneous generation of prions and
598 transmissible PrP amyloid in a humanised transgenic mouse model of A117V GSS. *PLoS*
599 *Biol.* 2020 Jun 9;18(6):e3000725. doi: 10.1371/journal.pbio.3000725. PMID: 32516343;
600 PMCID: PMC7282622.
- 601 33. Marín-Moreno A, Espinosa JC, Torres JM. Transgenic mouse models for the study of
602 prion diseases. *Prog Mol Biol Transl Sci.* 2020;175:147-177. doi:
603 10.1016/bs.pmbts.2020.08.007. Epub 2020 Sep 11. PMID: 32958231.
- 604 34. Torres JM, Castilla J, Pintado B, et al. Spontaneous generation of infectious prion
605 disease in transgenic mice. *Emerg Infect Dis.* 2013 Dec;19(12):1938-47. doi:
606 10.3201/eid1912.130106. PMID: 24274622; PMCID: PMC3840888.
- 607 35. Yang W, Cook J, Rassbach B, et al. A New Transgenic Mouse Model of Gerstmann-
608 Straussler-Scheinker Syndrome Caused by the A117V Mutation of PRNP. *J Neurosci.* 2009
609 Aug 12;29(32):10072-80. doi: 10.1523/JNEUROSCI.2542-09.2009. PMID: 19675240;
610 PMCID: PMC2749997.
- 611 36. Asante EA, Linehan JM, Smidak M, et al. Inherited prion disease A117V is not
612 simply a proteinopathy but produces prions transmissible to transgenic mice expressing
613 homologous prion protein. *PLoS Pathog.* 2013;9(9):e1003643. doi:
614 10.1371/journal.ppat.1003643. Epub 2013 Sep 26. PMID: 24086135; PMCID: PMC3784465.
- 615 37. Senesi M, Lewis V, Kim JH, et al. In vivo prion models and the disconnection
616 between transmissibility and neurotoxicity. *Ageing Res Rev.* 2017 Jul;36:156-164. doi:
617 10.1016/j.arr.2017.03.007. Epub 2017 Apr 24. PMID: 28450269.

618 **Figure legends**

619 **Figure 1 Genetic pedigrees (A)** Visual representation of the R136S Spanish family history.
620 **(B)** Visual representation of the homozygous R136S Portuguese family (inferred from
621 Pacheco et al.¹⁴). Created with BioRender.com

622 **Figure 2 Magnetic resonance imaging scan of the index patient.**

623 **Figure 3 Neuropathological characterization. (A1)** Frontal cortex shows prominent
624 neuronal loss and gliosis with loss of cortical structure and mild superficial spongiosis (H&E
625 stain). **(A2)** anti-PrP immunohistochemistry (12F10 antibody) shows a very high density of
626 multicentric PrP plaques covering the whole cortical thickness. **(A3)** These large multicentric
627 plaques are well identified in the PAS stain and the clusters of large amyloid plaques are
628 observed by immunohistochemistry with the 12F10 anti-PrP antibody **(A4)**. **(A5)**
629 Immunohistochemistry for hyperphosphorylated tau shows marked dystrophic neurites
630 surrounding the plaques in the hippocampus (AT8 immunohistochemistry). **(A6)** Abundant
631 multicentric plaques are detected in the molecular layer of the cerebellum (anti-PrP
632 immunostaining, 12F10 antibody).

633 **Figure 4 Western blotting with the 3F4 antibody of fresh-frozen tissue from the**
634 **PrP^{Pres}R136S index patient.** Multiple bands with low molecular weight bands of approximately
635 8kDa in contrast to sCJDMM1. Westerns blots of CTR - PK+ (1), CTR - PK- (2),
636 PrPresR136S Spanish proband frontal cortex (3), temporal cortex (4), parietal cortex (5),
637 occipital cortex (6), hippocampus (7), thalamus (8), cerebellum (9), frontal cortex with
638 PNGaseF+ (10), temporal cortex with PNGaseF+ (11) and sCJDMM1 (12) demonstrate that
639 all fractions (3-11) have abnormal patterns of PrPres. All regions except for occipital cortex
640 display a multiple band pattern.

641 **Figure 5 *In vitro* human misfolded PrP propagation by recPMCA using R136 vs. S136**
642 **human as substrates.** Human 129M 136R (wt) rec-PrP, human 129M 136S rec-PrP and a
643 mix of both rec-PrPs in ratio 1:1 were complemented with chicken brain homogenate, seeded
644 with different dilutions of recPMCA-adapted CJD MM1 misfolded rec-PrP (10⁻¹ – 10⁻⁸) and
645 subjected to a unique 24 h round of standard recPMCA. Amplified samples were digested
646 with 50 µg/ml of Proteinase-K and analyzed by western blot using monoclonal antibody D18
647 (1:5,000). No significant differences were found in the propagation ability of the R136 (wt)
648 vs. the mutant R136S rec-PrP or the mix 1:1 of both proteins.

649 **Figure 6 Spontaneous generation of human misfolded recombinant proteins.** Graphical
650 representation of the emergence of spontaneous protein misfolding evaluated through
651 Western blot analysis in SDS-PAGE for each round of recPMCA (outlined as R01–R15).
652 Different 129M human recombinant proteins were grouped according to the substitution.
653 Every experiment contained four tubes (intra-experimental duplicates) and was performed in
654 duplicate as shown. The percentage of positive tubes (tubes showing a protease resistant
655 signal after digestion with 80 mg/ml of PK) after each round of recPMCA was noted with
656 different intensities of grey, as shown in the legend below the figure. Neither wild-type (wt)
657 129M nor R136S 129M were able to misfold spontaneously. WT: wild type human rec-PrP^{Sc}.

Figures

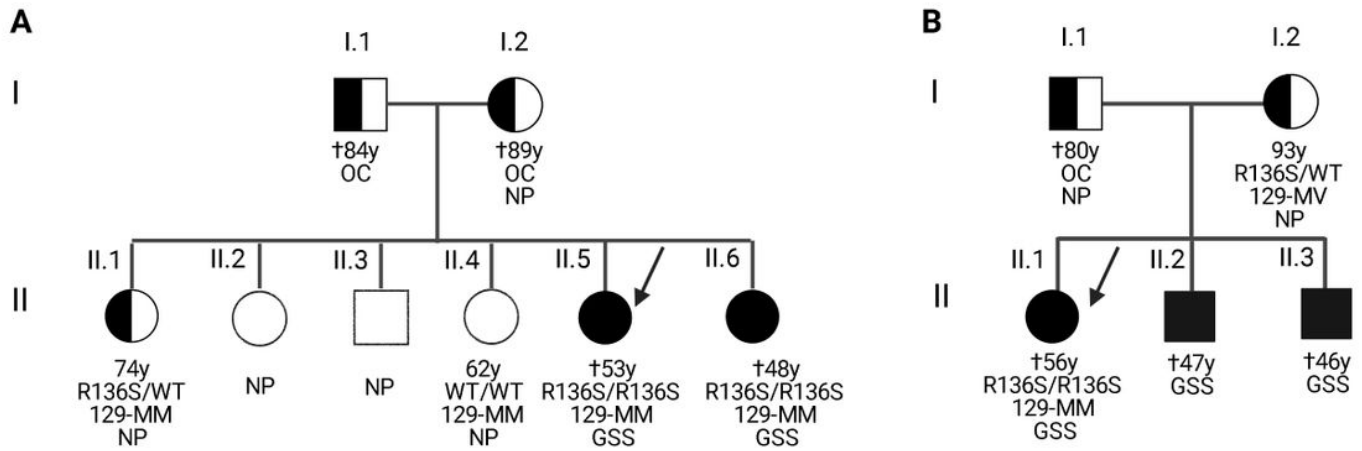


Figure 1

Genetic pedigrees (A) Visual representation of the R136S Spanish family history. (B) Visual representation of the homozygous R136S Portuguese family (inferred from 620 Pacheco et al. 14). Created with BioRender.com

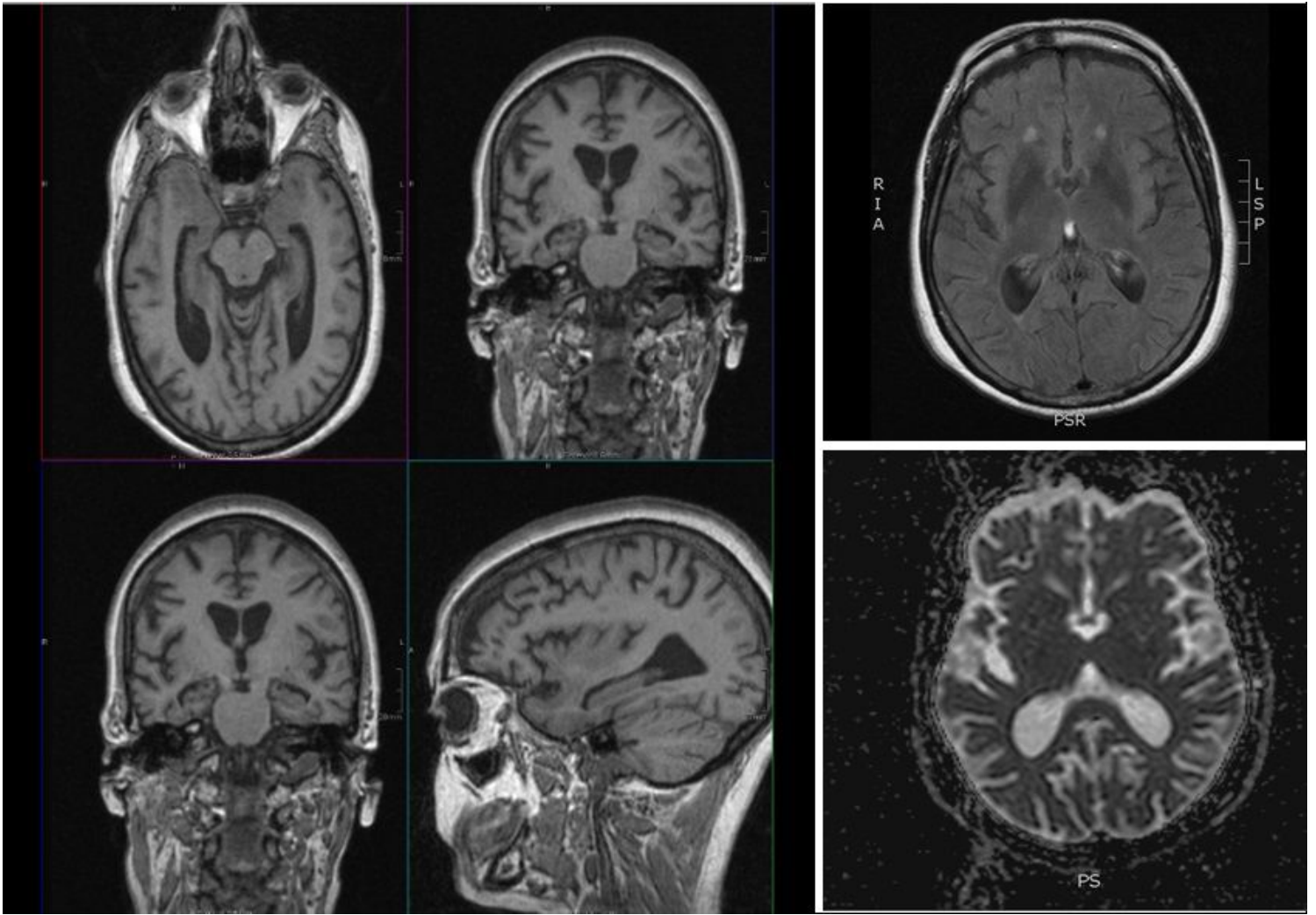


Figure 2

Magnetic resonance imaging scan of the index patient.

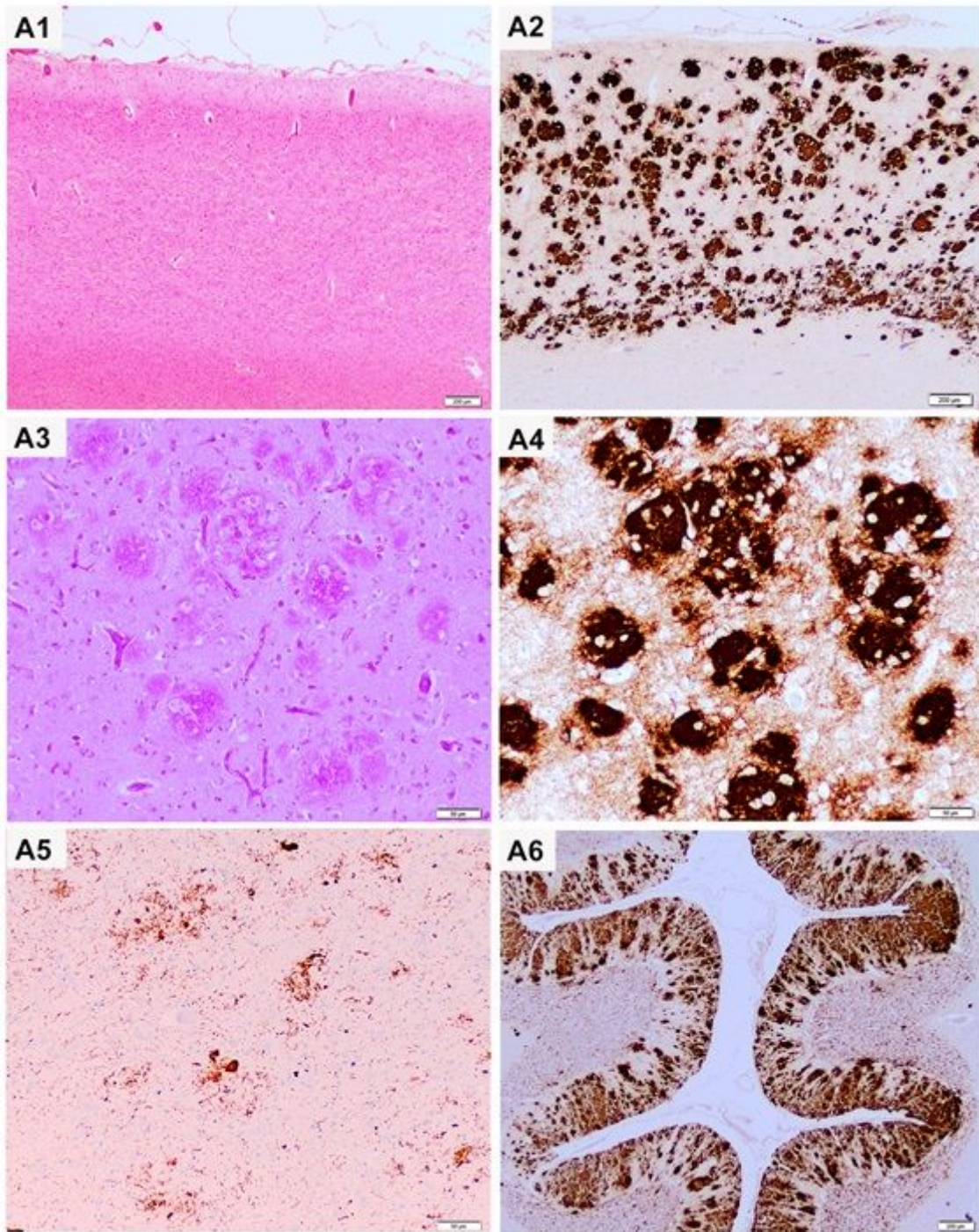


Figure 3

Neuropathological characterization. (A1) Frontal cortex shows prominent neuronal loss and gliosis with loss of cortical structure and mild superficial spongiosis (H&E stain). (A2) anti-PrP immunohistochemistry (12F10 antibody) shows a very high density of multicentric PrP plaques covering the whole cortical thickness. (A3) These large multicentric plaques are well identified in the PAS stain and the clusters of large amyloid plaques are observed by immunohistochemistry with the 12F10 anti-PrP antibody (A4). (A5) Immunohistochemistry for hyperphosphorylated tau shows marked dystrophic neurites surrounding the plaques in the hippocampus (AT8 immunohistochemistry). (A6) Abundant

multicentric plaques are detected in the molecular layer of the cerebellum (anti-PrP immunostaining, 12F10 antibody).

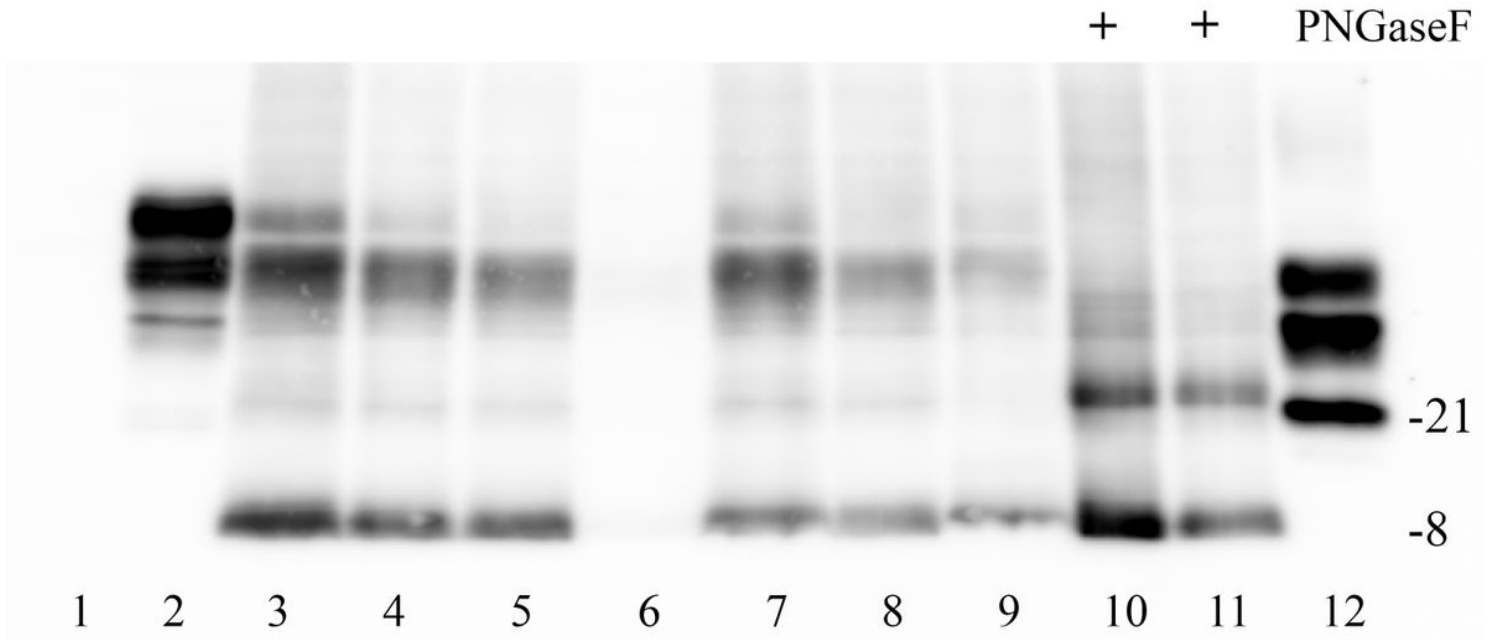


Figure 4

Western blotting with the 3F4 antibody of fresh-frozen tissue from the PrPresR136S index patient. Multiple bands with low molecular weight bands of approximately 8kDa in contrast to sCJDMM1. Westerns blots of CTR - PK+ (1), CTR - PK- (2), PrPres136s Spanish proband frontal cortex (3), temporal cortex (4), parietal cortex (5), occipital cortex (6), hippocampus (7), thalamus (8), cerebellum (9), frontal cortex with PNGaseF+ (10), temporal cortex with PNGaseF+ (11) and sCJDMM1 (12) demonstrate that all fractions (3-11) have abnormal patterns of PrPres. All regions except for occipital cortex display a multiple band pattern.

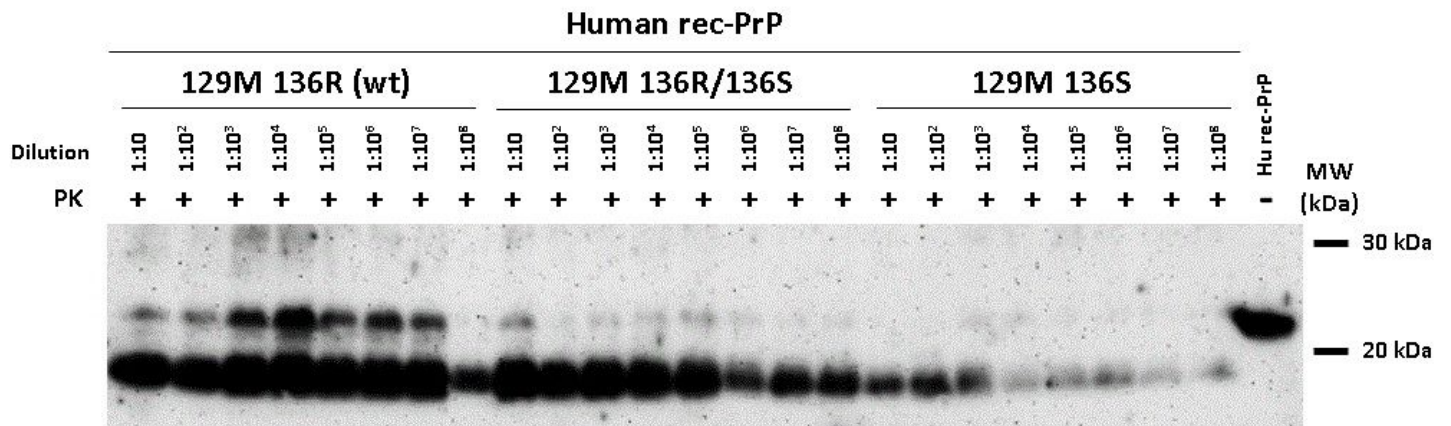


Figure 5

In vitro human misfolded PrP propagation by recPMCA using R136 vs. S136 human as substrates. Human 129M 136R (wt) rec-PrP, human 129M 136S rec-PrP and a mix of both rec-PrPs in ratio 1:1 were complemented with chicken brain homogenate, seeded with different dilutions of recPMCA-adapted CJD MM1 misfolded rec-PrP (10^{-1} – 10^{-8}) and subjected to a unique 24 h round of standard recPMCA. Amplified samples were digested with 50 μ g/ml of Proteinase-K and analyzed by western blot using monoclonal antibody D18 (1:5,000). No significant differences were found in the propagation ability of the R136 (wt) vs. the mutant R136S rec-PrP or the mix 1:1 of both proteins.

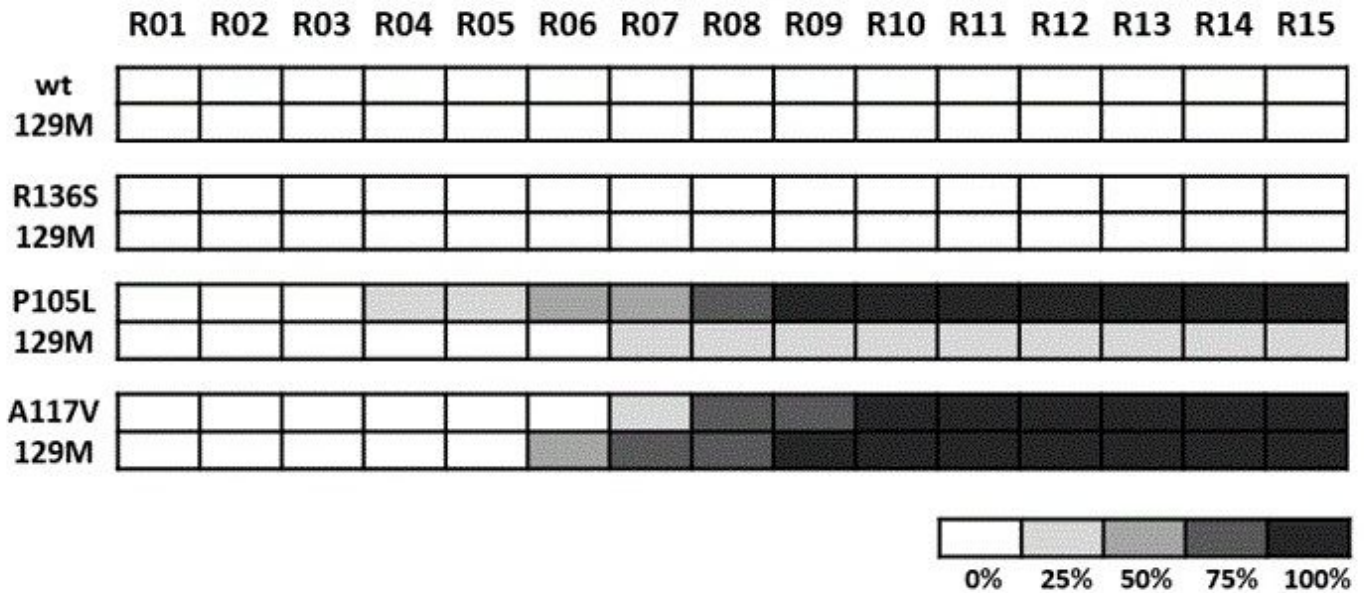


Figure 6

Spontaneous generation of human misfolded recombinant proteins. Graphical representation of the emergence of spontaneous protein misfolding evaluated through Western blot analysis in SDS-PAGE for each round of recPMCA (outlined as R01–R15). Different 129M human recombinant proteins were grouped according to the substitution. Every experiment contained four tubes (intra-experimental duplicates) and was performed in duplicate as shown. The percentage of positive tubes (tubes showing a protease resistant signal after digestion with 80 mg/ml of PK) after each round of recPMCA was noted with different intensities of grey, as shown in the legend below the figure. Neither wild-type (wt) 129M nor R136S 129M were able to misfold spontaneously. WT: wild type human rec-PrPSc